International Journal of Electrochemical Science 19 (2024) 100555

Contents lists available at ScienceDirect

International Journal of Electrochemical Science

journal homepage: www.editorialmanager.com/ijoes

Electrochemical CO_2 conversion in eutectic Li-Ba and Li-Ca carbonate mixtures

Emma Laasonen [a,*], Anafi Nur'Aini [b], Alireza Charmforoushan [c], Vesa Ruuskanen [b], Markku Niemelä [b], Tuomas Koiranen [a], Jero Ahola [b], Jyrki M. Mäkelä [c]

[a] School of Engineering Science, LUT University, Lappeenranta, Finland
[b] School of Energy Systems, LUT University, Lappeenranta, Finland
[c] Aerosol Physics Laboratory, Faculty of Engineering and Natural Sciences, Tampere University, Tampere, Finland

ARTICLE INFO

Keywords:
Molten carbonate electrolysis
Carbon capture and utilization
Electrochemical reduction
Electrochemical conversion
Voltage efficiency

ABSTRACT

Here, the impact of electrolyte selection and electrolysis temperature on carbon morphology, energy consumption, and voltage efficiency in molten Li_2CO_3-$BaCO_3$ and Li_2CO_3-$CaCO_3$ electrolytes during 90 min 10 A constant current electrolysis are investigated. The scarcity of experimental investigations into these binary electrolytes, coupled with a lack of systematic investigation of temperature effects, necessitates further examination. The comprehensive analysis of the produced carbon reveals that both electrolyte composition and temperature influence carbon morphology. At lower temperatures the effect of electrolyte composition to the morphology is a more significant. The type and amount of metallic impurities mixed with the carbon vary depending on the electrolyte composition and electrolysis temperatures. The results from Li_2CO_3-$CaCO_3$ electrolyte show more promising compared to results from Li_2CO_3-$BaCO_3$ electrolyte in terms of product quality. Regarding electrolysis power and voltage efficiency, Li_2CO_3-$CaCO_3$ proves equal or superior to other electrolytes, depending on temperature. Heat generation occurs in all the experiments, which emphasizes the importance maintaining a constant electrolysis temperature in industrial processes to manage heat generation effectively.

1. Introduction

Molten carbonate electrolysis has been proved to be a feasible method to convert CO_2 to elementary carbon with various different morphologies. Based on various experimental works published within the last 15 years, including but not limited to [1–4–7], Li_2CO_3 is the most prominent electrolyte for this application. Besides pure Li_2CO_3, the suitability of various carbonate mixtures has been studied. Wu et al. [8], Le Van et al. [9] and Tang et al. [10] studied carbon production Li_2CO_3-Na_2CO_3-K_2CO_3. All of their results showed that by changing temperature has an effect on the size and shape of the product. However, no distinct dominant morphologies were observed. Similar results were obtained by Ijije et al. [11] in Li_2CO_3-K_2CO_3 electrolyte. More prominent results in terms of product quality have been obtained in Li_2CO_3-Na_2CO_3 electrolyte, as nanotubes can be produced [8,12]. Low concentration of Na_2CO_3 was more suitable, as the nanotube yield decreased when the proportional amount of Na_2CO_3 increased [8]. Nanotubes can also be produced in Li_2CO_3-$BaCO_3$ electrolyte [8,13]. Compared to the nanotubes produced in pure Li_2CO_3, nanotubes produced in Li_2CO_3-$BaCO_3$ were larger and more versatile in terms of the tube diameter. [8] Besides Li_2CO_3-$BaCO_3$, Li et al. [13] produced nanotubes in Li_2CO_3-$CaCO_3$ and Li_2CO_3-$SrCO_3$. Ren et al. [14] observed that when $CaCO_3$ is added to Li_2CO_3, some carbon nanotubes are produced, while majority of the product is amorphous. Compared to the tubes produced in pure Li_2CO_3, the tubes produced in Li_2CO_3-$CaCO_3$ are notably thinner. Ren et al. [14] also studied a mixture of Li_2CO_3 and $MgCO_3$. In this mixture the produced carbon had a honeycomb-like structure, and only a few tubes were observed.

Based on thermodynamic data and calculated deposition potentials in [15], it can be determined whether carbon or metal is deposited during the electrolysis. Accordingly the carbonates that could be utilized in carbon production by molten salt electrolysis are Li_2CO_3, $MgCO_3$, $CaCO_3$, $SrCO_3$, and $BaCO_3$. With other alkali metal and earth alkali metal carbonates metal deposition is more favourable, thus their utilization would cause side reactions. Out of these feasible options Li_2CO_3-$BaCO_3$ and Li_2CO_3-$CaCO_3$ were selected, as their proposed reaction

* Corresponding author.
E-mail address: emma.laasonen@lut.fi (E. Laasonen).

https://doi.org/10.1016/j.ijoes.2024.100555
Received 9 February 2024; Received in revised form 14 March 2024; Accepted 19 March 2024
Available online 20 March 2024

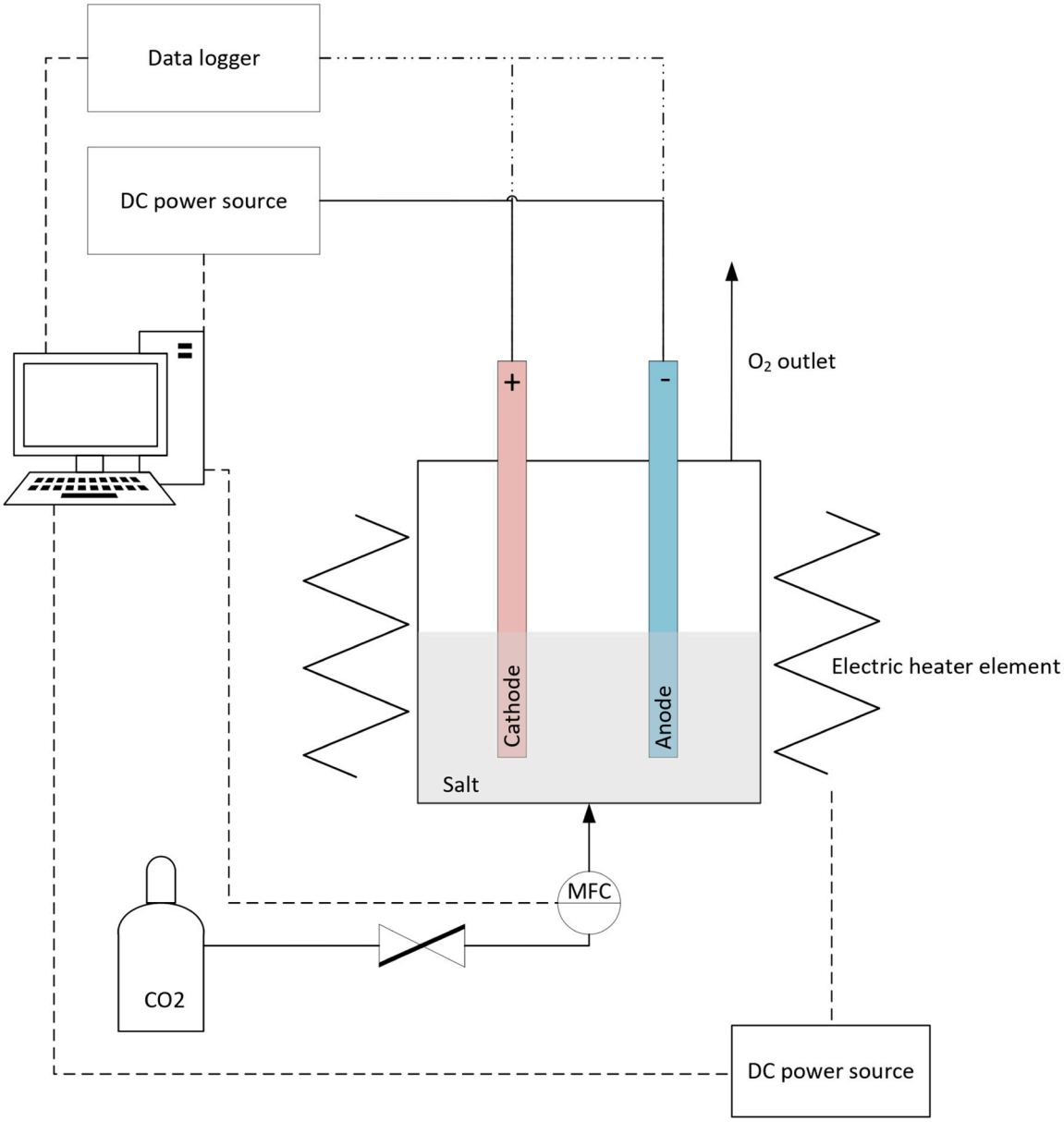

Fig. 1. Illustration of the electrolyzer setup.

Table 1
Specifications of equipment, controllers and measurement devices used.

Oven	Custom from Meyer vastus
Oven power source	EA-PSI 9500–30
Electrolysis power source	Rohde & Schwarz NGP-804
Data acquisition and logging multimeter	Keithley DAQ6150
Mass flow controller	Bronkhorst F-201DV-AGD-33-V MFC
Thermocouples	Jumo K type, DIN 43710
Control software	LabVIEW 2020 by NI
MFC communication	Beckhoff EK9000 with EtherCat I/O terminals

mechanisms (see Chapter 2.1) are different from each other and thus their effect on the produced carbon or energy consumption could be different. The scarcity of previous studies related to electrochemical carbon production in Li_2CO_3-$BaCO_3$ and Li_2CO_3-$CaCO_3$ mixtures leaves room for further examination. Li et al. [13] have studied both of these mixtures, and Li et al. [16] and Wu et al. [8]Li_2CO_3-$BaCO_3$ mixture, but all with only one temperature, while in the study presented here various electrolysis temperatures were investigated.

In general, there is a scarcity of studies specifically examining the impact of electrolysis temperature, creating an opportunity for additional research. According to [8,17–19] increasing electrolysis temperature in Li_2CO_3-Na_2CO_3-K_2CO_3 is affecting the produced carbon morphology. To the author's knowledge, no existing studies have explored the effect of electrolysis temperature in binary carbonate mixtures. Based on results obtained with ternary electrolytes it is reasonable to hypothesize that similar effects may manifest in binary electrolytes.

As previous studies concerning salt mixtures as an electrolyte have merely been focusing on the morphology of the produced carbon, here the electrolysis power, voltage efficiency, and energy consumption are discussed as well. These results are then compared with those of electrolysis conducted using pure Li_2CO_3. These factors play a key role in assessing the potential scalability of the process and are essential considerations for determining its feasibility.

2. Materials and methods

2.1. Reaction mechanism

Throughout the years various reaction mechanisms of carbon production from CO_2 by molten carbonate electrolysis have been presented. A clear consensus regarding the accurate mechanisms and reactions has yet to be established. According to [20], the splitting of Li_2CO_3 and $BaCO_3$ are similar,

$$Li_2CO_3 \rightarrow Li_2O + C + O_2 \quad (1)$$

and

$$BaCO_3 \rightarrow BaO + C + O_2. \quad (2)$$

With $CaCO_3$ the mechanism is different, mainly due to the limited CaO solubility [20].

$$3\ CaCO_3 \rightarrow 3\ CaO + C + 2\ CO_2 + O_2. \quad (3)$$

The mechanism of Eq. (1) and Eq. (2) has originally been presented by [21], while the mechanism of Eq. (3) by [22] and [23].

These presented total reactions include two electrochemical reactions, anodic and cathodic. The proposed cathodic reactions of Eq. (1), Eq. (2) and Eq. (3) are the same.

$$CO_3^{2-} + 4\ e^- \rightarrow C + 3\ O^{2-}. \quad (4)$$

Noteworthy is that a negative carbonate ion cannot migrate to the cathode by itself, it must be in a form of chargeless carbonate molecule, i.e. Li_2CO_3, leading to the reaction of

$$Li_2CO_3 + 4\ e^- \rightarrow C + Li_2O + 2O^{2-}. \quad (5)$$

The anodic reaction of Eq. (1) are Eq. (2)

$$O^{2-} \rightarrow 1/2O_2, \quad (6)$$

while the anodic reaction of Eq. (3) is proposed to be

$$CO_3^{2-} \rightarrow CO_2 + 1/2O_2 + 2e^-. \quad (7)$$

In addition to the electrochemical reactions, as chemical reaction where produced oxide is replenished back to carbonate

$$O^{2-} + CO_2 \rightarrow CO_3^{2-}. \quad (8)$$

is occurring.

2.2. Energy consumption and voltage efficiency

Electrolysis power can be calculated based on Eq. (9) in the case of direct current (DC)

$$P = UI, \quad (9)$$

when cell voltage is measured. Further, energy consumption of the electrolysis can be calculated

$$E = Pt, \quad (10)$$

where t is electrolysis time in seconds.

Voltage efficiency, a, of the process can be determined by comparing the measured cell voltage with thermoneutral voltage U_{tn} as

$$\eta_U = \frac{U_{tn}}{U}. \quad (11)$$

Thermoneutral voltage of this process is 1.02 V [2]. With known current efficiency overall efficiency of the process could be further determined.

The heat generated by electrolysis process can calculated as following based on the measured cell voltage and current and the thermoneutral voltage, which is the cell voltage corresponding the state

Table 2
Experiments conducted with eutectic Li_2CO_3-$BaCO_3$ 80:20 mol% and Li_2CO_3-$CaCO_3$ 80:20 mol% electrolytes.

Salt	T [°C]	i [A/cm^2]	I [A]	t [min]	$\dot{V}_{CO_2}$ [ml/min]	No. of repetitions
Li_2CO_3	750	0.2	10	90	40	1
Li_2CO_3-$BaCO_3$	700	0.2	10	90	40	2
Li_2CO_3-$BaCO_3$	725	0.2	10	90	40	2
Li_2CO_3-$BaCO_3$	750	0.2	10	90	40	2
Li_2CO_3-$BaCO_3$	775	0.2	10	90	40	2
Li_2CO_3-$CaCO_3$	700	0.2	10	90	40	2
Li_2CO_3-$CaCO_3$	725	0.2	10	90	40	2
Li_2CO_3-$CaCO_3$	750	0.2	10	90	40	2
Li_2CO_3-$CaCO_3$	775	0.2	10	90	40	2

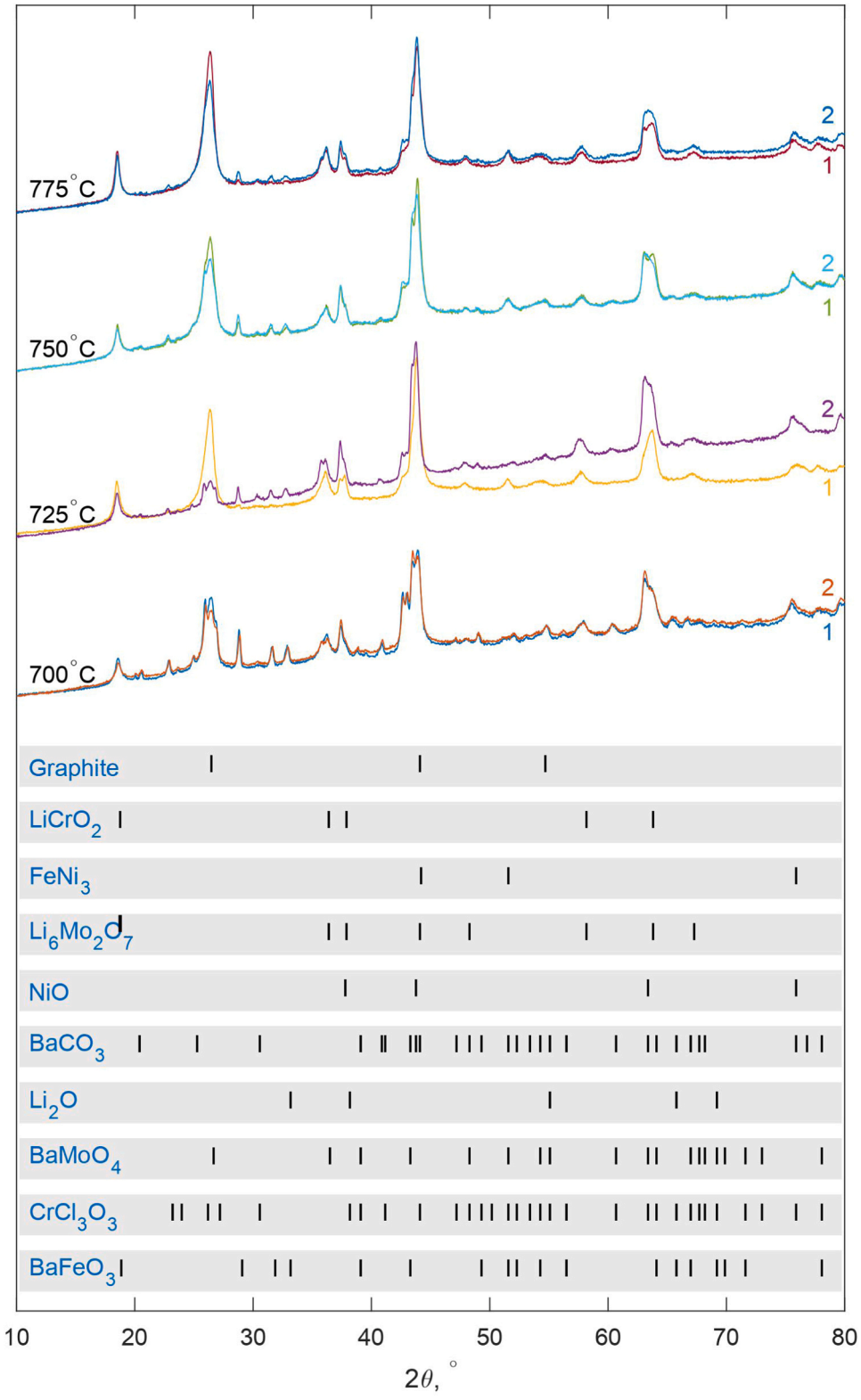

Fig. 2. XRD diffraction patterns of carbon samples produced at different temperatures in Li_2CO_3-$BaCO_3$ electrolyte. Number on the right side of the figure is equal to the number of the repetition.

Table 3
Phase composition analysis (w%) of the samples from Li_2CO_3-$BaCO_3$ electrolyte based on reference intensity ratio (RIR) analysis.

Sample	Graphitic C	$LiCrO_2$	$FeNi_3$	$Li_6Mo_2O_7$	NiO	$BaCO_3$	Li_2O	$BaMoO_4$	Cl_3CrO_3	$BaFeO_3$	Unidentified component
Li_2CO_3-$BaCO_3$ 700, rep1	36.4	11.8	5.1	6.2	8.4	-	14.3	2.2	8.0	6.1	1.7
Li_2CO_3-$BaCO_3$ 700, rep2	35.4	13.6	6.7	16.3	7.8	2.4	8.0	5.4	2.9	1.6	0.8
Li_2CO_3-$BaCO_3$ 725, rep1	60.7	14.0	2.4	13.4	2.5	-	-	4.8	1.4	0.8	0.2
Li_2CO_3-$BaCO_3$ 725, rep2	16.1	20.0	15.9	25.3	8.1	4.8	4.2	2.5	2.0	1.1	0.5
Li_2CO_3-$BaCO_3$ 750, rep1	57.9	10.0	5.4	12.9	3.1	1.9	1.8	6.4	-	0.7	0.1
Li_2CO_3-$BaCO_3$ 750, rep2	51.6	3.4	7.8	16.4	10.5	2.2	1.3	3.9	2.2	0.7	1.4
Li_2CO_3-$BaCO_3$ 775, rep1	58.1	12.1	7.1	14.6	1.2	-	-	6.7	-	0.3	0.2
Li_2CO_3-$BaCO_3$ 775, rep2	52.0	3.4	7.2	18.0	5.5	-	2.7	9.4	1.1	0.5	0.8

where heat is neither produced or consumed by the overall reaction.

$$P_{heat} = (U - U_{tn})I. \quad (12)$$

2.3. Reactor unit

The active areas i.e the area in the salt of both anode and cathode were made of Inconel Alloy HX (Alloy X), a Ni-Cr-Fe-Mo alloy, from Harald Pihl (https://www.haraldpihl.com/). According to the manufacturer's datasheet this material has a high corrosion resistance up to 1200 °C, hence this material was selected. Due to the high cost of Alloy X the part of the electrode above salt was made of stainless steel 316. The active surface area of the anode and cathode in the molten salt was 50 cm^2. Salt mixtures utilized in the experimental work were Li_2CO_3-$BaCO_3$ 80:20 mol% and Li_2CO_3-$CaCO_3$ 80:20 mol%. Experimental setup is illustrated in Fig. 1, and measuring and control units of the setup are listed in Table 1.

2.4. Procedure

Electrodes were placed inside the molten salt at desired temperature (Table 2). Additionally to the experiments with Li_2CO_3-$BaCO_3$ 80:20 mol% and Li_2CO_3-$CaCO_3$ 80:20 mol% mixtures, one experiment with pure Li_2CO_3 was conducted for comparison and a reference. CO_2 feed was turned on, and the 10 A constant current electrolysis was run for 90 min. Temperature range of the experiments was selected with the consideration of the melting points. Based on temperature measurements the oven temperature remained within 1 °C from the set point throughout the electrolysis. Temperature measurements obtained with data acquisition and logging multimeter Keithley DAQ6150 were utilized to control heating power to maintain desired temperature. CO_2 feed was calculated to be sufficient for the reaction in Eq. (8) to occur and thus prevent oxide accumulation.

Produced carbon was washed with HCl to remove salt residues. After washing the sample was rinsed with deionized water and dried in the oven at 105 °C.

2.5. Analysis methods

For examining distinct carbon morphologies scanning electron microscopy (SEM) was utilized. Additionally, energy-dispersive X-ray spectroscopy (EDS) was used to analyse possible metal residues mixed with the carbon. The field-emission scanning electron microscope (Zeiss UltraPlus) with an added energy-dispersive X-ray spectrometer (Oxford Instruments XMaxN 80) was applied for SEM and EDS analyses. X-ray diffraction (XRD) analysis was utilized to study the amorphousness of the carbon product and the compositions of impurities in the samples. The XRD analysis was performed with a Panalytical Empyrean multipurpose X-ray diffractometer (PANalytical B.V.) using monochromatized CuK_α radiation in the measurement range $10° < 2\theta < 80°$. Match! software by Crystal Impact was used to identify found peaks. Reference intensity ratio (RIR) was used to determine the phase composition (w%) of the samples.

3. Results and discussion

3.1. Product identification

3.1.1. Product from Li_2CO_3-$BaCO_3$ 80:20 mol% electrolyte

XRD patterns of all the samples produced in Li_2CO_3-$BaCO_3$ 80:20 mol% electrolyte is shown in Fig. 2. Based on the XRD patterns it is evident that a significant number of different impurity components are present in the samples. Graphitic carbon has main peaks at around 26.2°, 43.8°, and 54.4°, while all the other found peaks originate from various impurities. Found impurity components are $LiCrO_2$, $FeNi_3$, $Li_6Mo_2O_7$, NiO, $BaCO_3$, Li_2O, $BaMoO_4$, Cl_3CrO_3, and $BaFeO_3$. Lithium and barium originate from the electrolyte, while chromium, iron, nickel and molybdenum originate from the electrodes. $BaCO_3$ is a direct salt residue not properly removed during washing. Chlorine from the HCl is reacting with chromium oxide during the sample washing, explaining the presence of chlorine in the samples.

The phase compositions of the samples, as indicated by the XRD results and detailed in Table 3, offer valuable insights about the impurity levels in the samples. Notably, the carbon content in the samples is, at best, below 60 %. This discovered high amount of impurities poses a significant challenge, as it negatively impacts the quality of the product, as previously discussed in [5]. The effect of metals catalysing and nucleation the growth of various carbon structures has previously been discussed e.g. by [4,24,25]. Noteworthy is that the type and quantity of impurities exhibit variations not only between experiments conducted at different temperatures but also among repetitions. This variability lacks a clear explanation, although similar trends regarding difference between repetitions have been observed in previous studies, as reported in [2,5]. To be able to determine the possible reason more experimental work is required.

The presence of Li_2O in the samples suggests inadequate regeneration with CO_2 to Li_2CO_3. With pure Li_2CO_3 electrolyte this regeneration process is fast, and no oxide accumulation should occur when CO_2 is constantly fed to the system at sufficient pace. It can be speculated that the addition of $BaCO_3$ is affecting the solubility of CO_2 and subsequently to the regeneration process negatively. Based on these results it could be concluded that utilization of this Li_2CO_3-$BaCO_3$ electrolyte is not a viable option in terms of achieving desired product purity and quality.

SEM images in of carbon produced in Li_2CO_3-$BaCO_3$ at different temperatures are shown in Fig. 3. Some clear differences are observed between the samples. According to XRD results all these forms of the carbon are graphitized. Carbon produced at 700 °C contain both spherical and irregular-shaped carbon structures with varying sizes and without one dominant structure. When temperature is increased to 725 °C merely spherical, onion-like, structures are found, similar to ones presented in [1,2,5,11,16,26,27]. Spherical structures are notably smaller compared to particles found from carbon produced at 700 °C. When temperature is further increased to 750 °C and 775 °C, tubular structures are present along some spherical structures. Previously tubular structures have been produced by this same method by [3,4,6,13,14,18,24,25,28,29]. Ren et al. [4] concluded at least Ni, Fe, Cu, and Co presence in the system contributes to the growth of tubular structures by nucleating the growth.

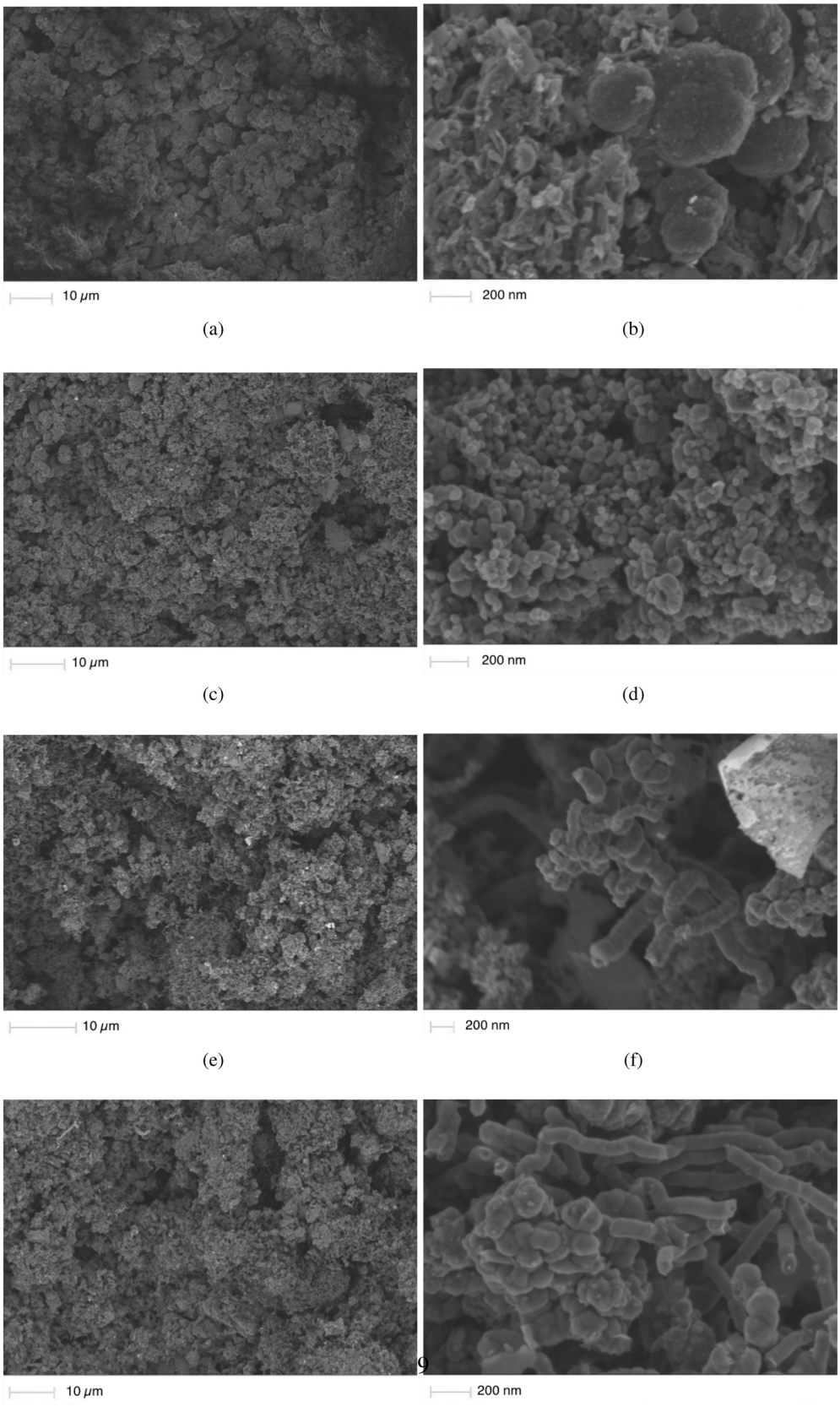

Fig. 3. Carbon produced at a)-b) 700 °C c)-d) 725 °C e)-f) 750 °C g)-h) 775 °C temperature in Li_2CO_3-$BaCO_3$ electrolyte. Electrolysis time in all the experiments was 90 min, and current density 0.2 A cm^{-2}.

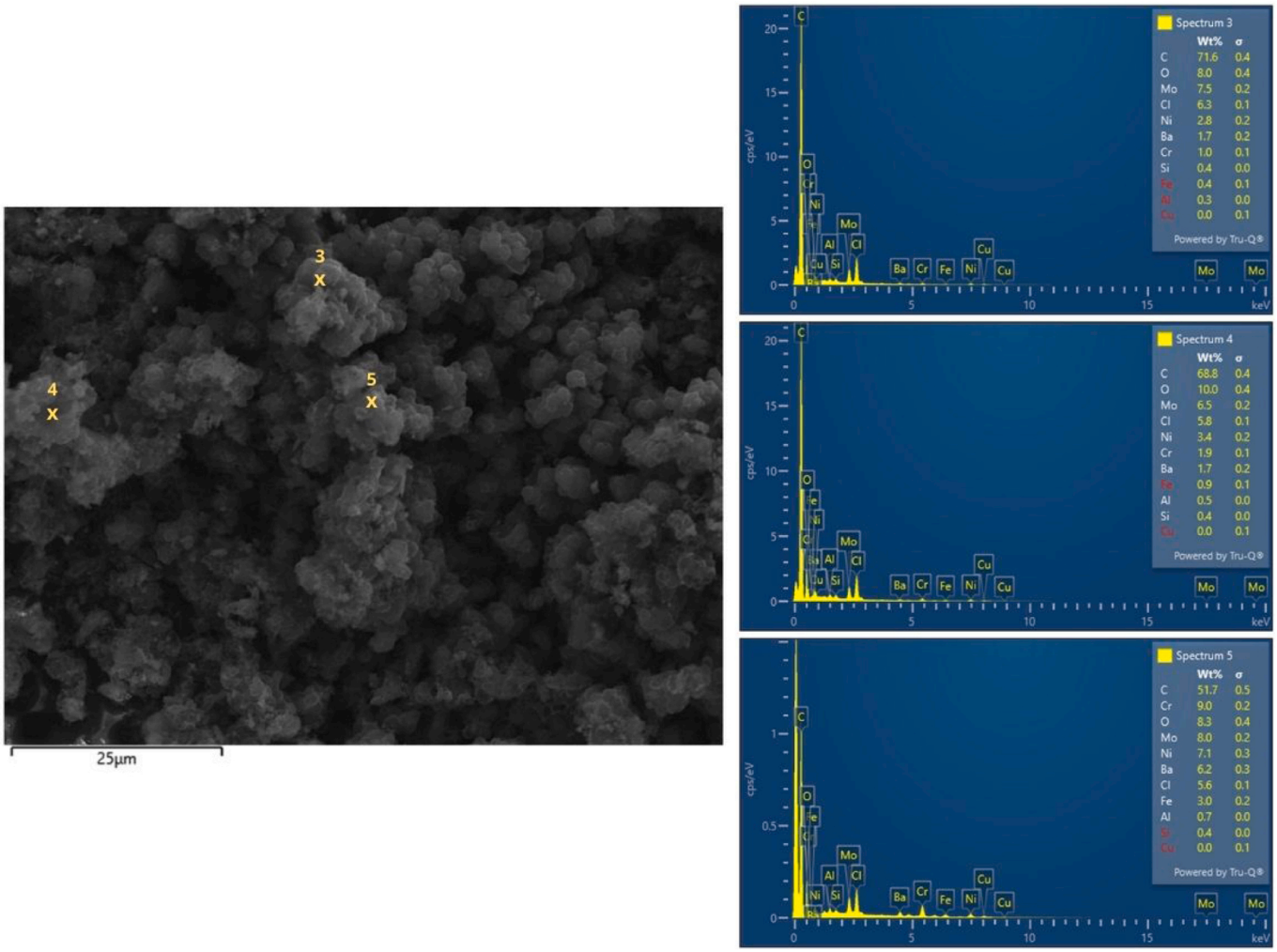

Fig. 4. EDS spectra of carbon produced in Li_2CO_3-$BaCO_3$ at 700 °C temperature.

Previous literature discussing about the effect of temperature, including [8,17–19], also observed that by increasing temperature the amount of tubular structures increased. Yu et al. [19] speculated that increasing temperature enhances fluidity, which would affect the interphase between electrolyte and cathodic surface and subsequently the product morphology. Wang et al. [18] speculated that by increasing temperature the electrochemical potential decreases and subsequently the carbon deposition could be accelerated. This could favour the growth of larger carbon particles.

EDS spectra of carbon produced in Li_2CO_3-$BaCO_3$ at different temperatures are shown in Figs. 4-7. Elements found with EDS are in line with the elements of components found with XRD, with the exception of lithium. Lithium found with XRD is not visible in EDS, as lithium is too light of an element to be detected. Nickel, chromium, iron and molybdenum found originate from the Alloy X electrodes. Barium is residues from the salt, and chloride is residues from washing. The heterogeneous nature of the sample composition is evident, as various spots within the same sample exhibit different EDS spectra.

EDS spectra of carbon produced in Li_2CO_3-$BaCO_3$ at 700 °C temperature are shown in Fig. 4, carbon produces.

EDS spectra of carbon produced in Li_2CO_3-$BaCO_3$ at 725 °C temperature are shown in Fig. 5.

EDS spectra of carbon produced in Li_2CO_3-$BaCO_3$ at 750 °C temperature are shown in Fig. 6.

EDS spectra of carbon produced in Li_2CO_3-$BaCO_3$ at 775 °C temperature are shown in Fig. 7.

3.1.2. *Product from Li_2CO_3-$CaCO_3$ 80:20 mol% electrolyte*

XRD diffraction patterns of all the samples produced in Li_2CO_3-$CaCO_3$ electrolyte is shown in Fig. 8 and phase compositions of the samples are shown in Table 4. Graphitic carbon has main peaks at around 26.2˚, 43.8˚, and 54.4˚. The amount of carbon varied between the samples, and at best it was almost 96 %. In addition to graphitic carbon metallic impurities, namely $LiCrO_2$, $FeNi_3$, $Li_6Mo_2O_7$, Fe_2O_3, chromium chloride hexahydrate, and ferrihydrite, were found in the samples. All metals of those impurities originate from the Alloy X electrodes, and are released due to corrosion, while hydrogen and chlorine originate from the HCl used in the sample washing.

Based on the results in Fig. 8 and Table 4 it can be concluded that electrolysis temperature is related to what metallic impurities are found mixed with the carbon, as phase compositions noticeably differ from each other when electrolysis is temperature changed. The differences between repetitions done at same temperature were minor, as same impurities were found but the amounts were slightly different. $Li_6Mo_2O_7$ and $LiCrO_2$ were found from all the samples, thought amount their amounts varied significantly between the samples. $FeNi_3$, chromium chloride hexahydrate (CCHH), and ferrihydrite (FH) were only present in some of the samples. Previously the presence of $LiCrO_2$ and $FeNi_3$ in carbon produced by electrochemical splitting of CO_2 in molten carbonate has been reported by [5].

Both chromium chloride hexahydrate (CCHH), and ferrihydrite (FH) are formed during the washing process, as the only possible source of hydrogen is HCl. They are likely to originate from chromium and iron

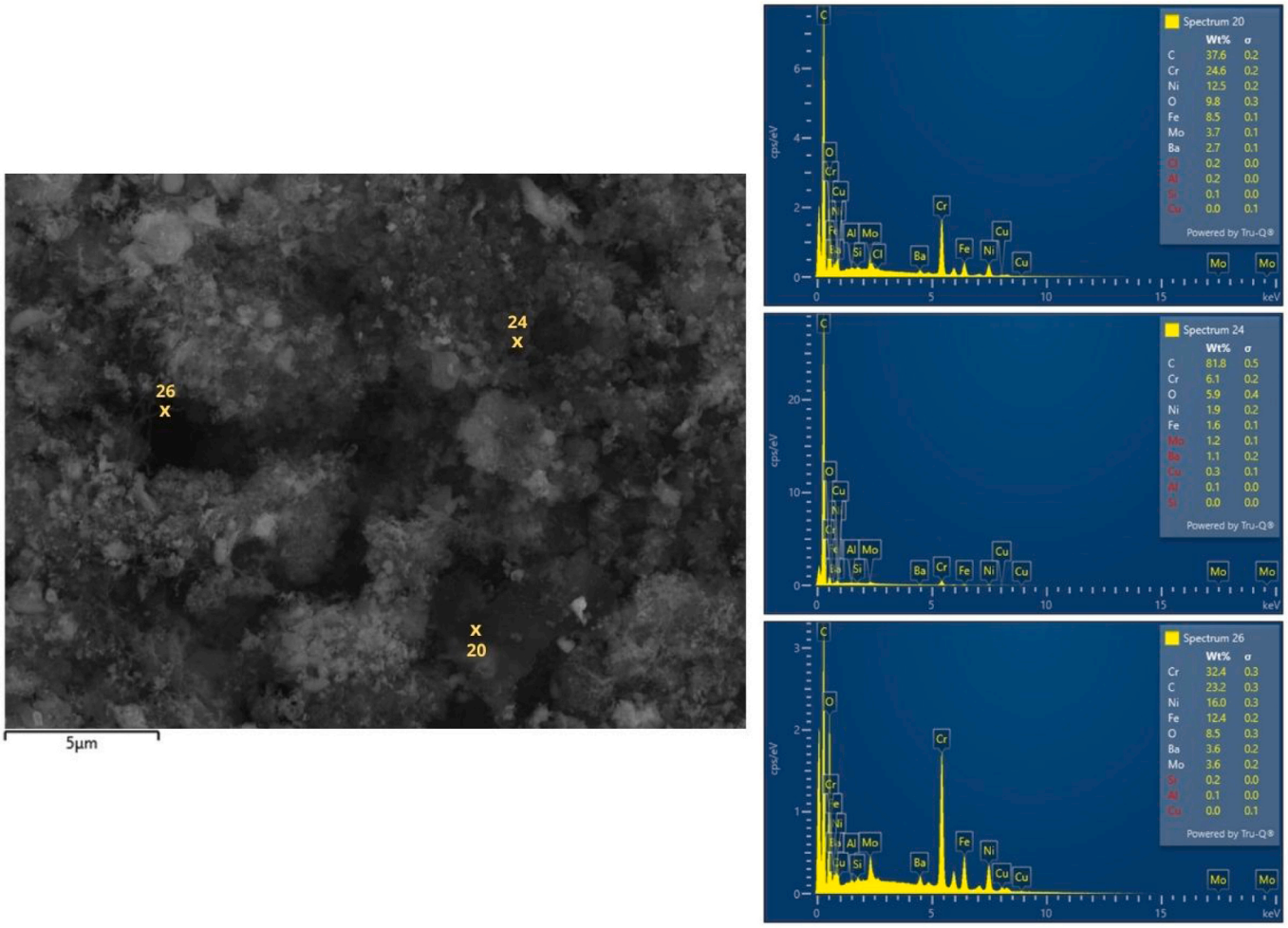

Fig. 5. EDS spectra of carbon produced in Li_2CO_3-$BaCO_3$ at 725 °C temperature.

oxides, which are formed during the electrolysis due to corrosion and oxygen production. Chromium chloride could be produced from Cr_2O_3 during the washing process as Cr_2O_3 is an amphoteric oxide [30]

$$Cr_2O_3 + 6\,HCl \rightarrow 3\,H_2O + 2\,CrCl_3, \quad (13)$$

which then further reacts to form chromium chloride hexahydrate.

The main peak found at around 26° is fairly wide and not symmetrical, especially in the carbon produced at 700 °C and 725 °C temperatures. This could be an indication that some smaller other, smaller peaks located near the graphite main peak (26.2°). Phase composition analysis in Table 4 revealed the existence of at least one unidentified component. It can be concluded that this unidentified component likely contributes to the peak observed at around 26°. Noteworthy is that unlike samples from the Li_2CO_3-$BaCO_3$ electrolyte, those from the Li_2CO_3-$CaCO_3$ electrolyte exhibit this distinctive wide peak. This implies that the impurity causing the observed peak is specific to the samples produced in Li_2CO_3-$CaCO_3$ electrolyte.

SEM images taken from carbon produced in Li_2CO_3-$CaCO_3$ electrolyte at different temperatures are shown in Fig. 9. Morphology of the carbon significantly changes when electrolysis temperature is changed. According to XRD results all these forms of the carbon are graphitized. Carbon produced at 700 °C has platelet-like sharp edges, and there are holes within the particle. Those found holes have likely been filled with the electrolyte, which has been removed by washing with HCl. This type of carbon resembles carbon nano-scaffold reported in [12] and honey-comb reported in [8]. When temperature was increased to 725 °C, the carbon structure are more tightly packed, as no holes are found. Also, the edges of the particles are not as sharp as they are in the carbon produced at 750 °C.

At 750 °C temperature carbon morphology changes significantly compared to lower temperatures. Throughout the sample spherical, onion-like, structures are found. Similar spherical structures have previously been reported in [1,2,5,11,16,26,27]. When temperature is further increased to 750 °C, tubular structures are found along spherical, similarly as in the carbon produced in Li_2CO_3-$BaCO_3$.

EDS spectra of carbon produced in Li_2CO_3-$CaCO_3$ at different temperatures are shown in Figs. 10-13. Again, elements found with EDS correlate with the elements of the components found with XRD, with the exception of lithium. Nickel, chromium, iron and molybdenum found originate from the Alloy X electrodes, and according to XRD they form components such as $LiCrO_2$, $FeNi_3$, and $Li_6Mo_2O_7$. Chloride originates from the HCl and only gets on contact with the sample during the washing process. Calcium residues observed originate from $CaCO_3$ electrolyte. As different spots of the same sample have different EDS spectra is can be concluded that the samples are heterogeneous.

EDS spectra of carbon produced in Li_2CO_3-$CaCO_3$ at 700 °C temperature are shown in Fig. 10.

EDS spectra of carbon produced in Li_2CO_3-$CaCO_3$ at 725 °C temperature are shown in Fig. 11.

EDS spectra of carbon produced in Li_2CO_3-$CaCO_3$ at 750 °C temperature are shown in Fig. 12.

EDS spectra of carbon produced in Li_2CO_3-$CaCO_3$ at 775 °C temperature are shown in Fig. 13.

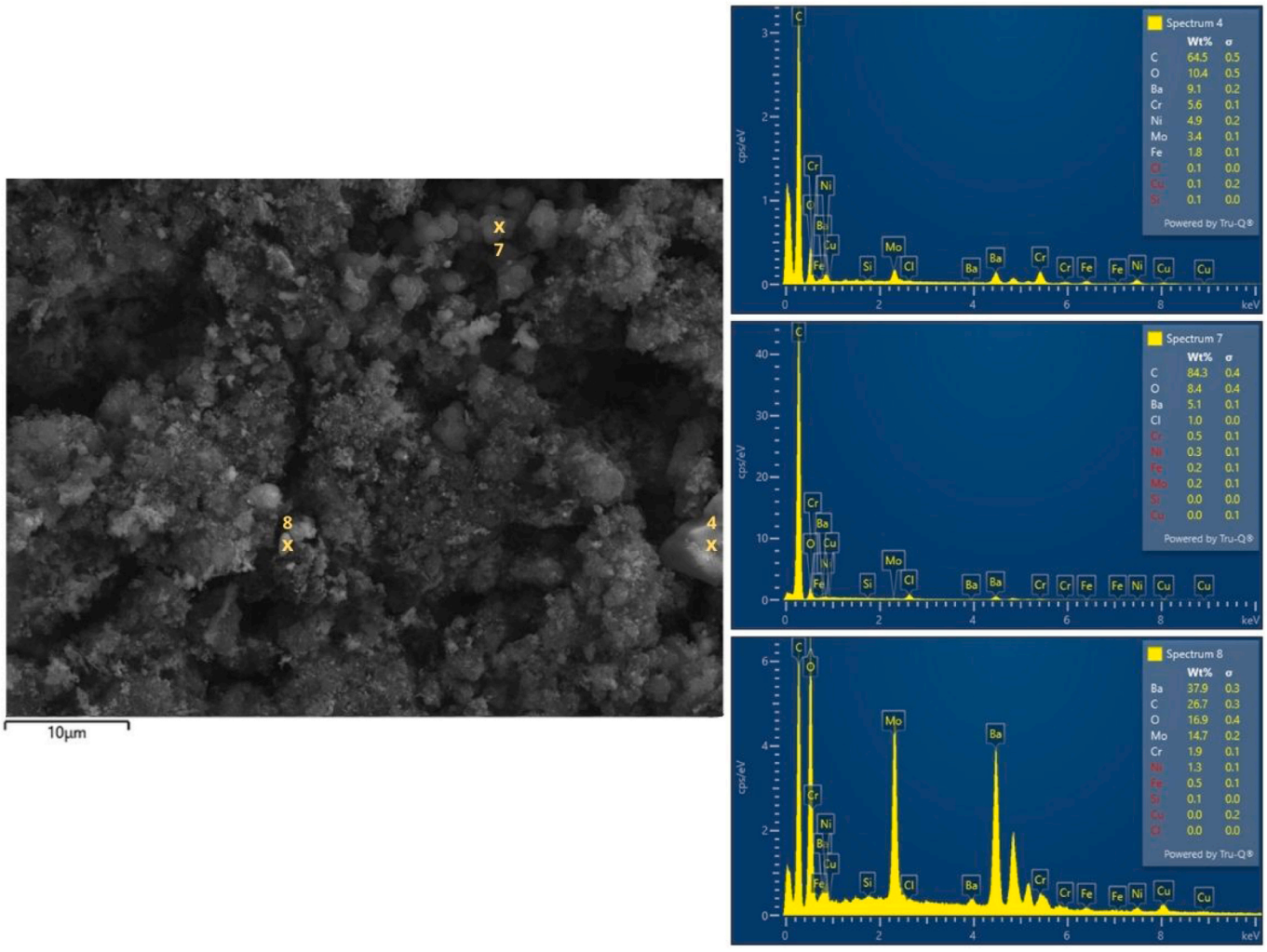

Fig. 6. EDS spectra of carbon produced in Li_2CO_3-$BaCO_3$ at 750 °C temperature.

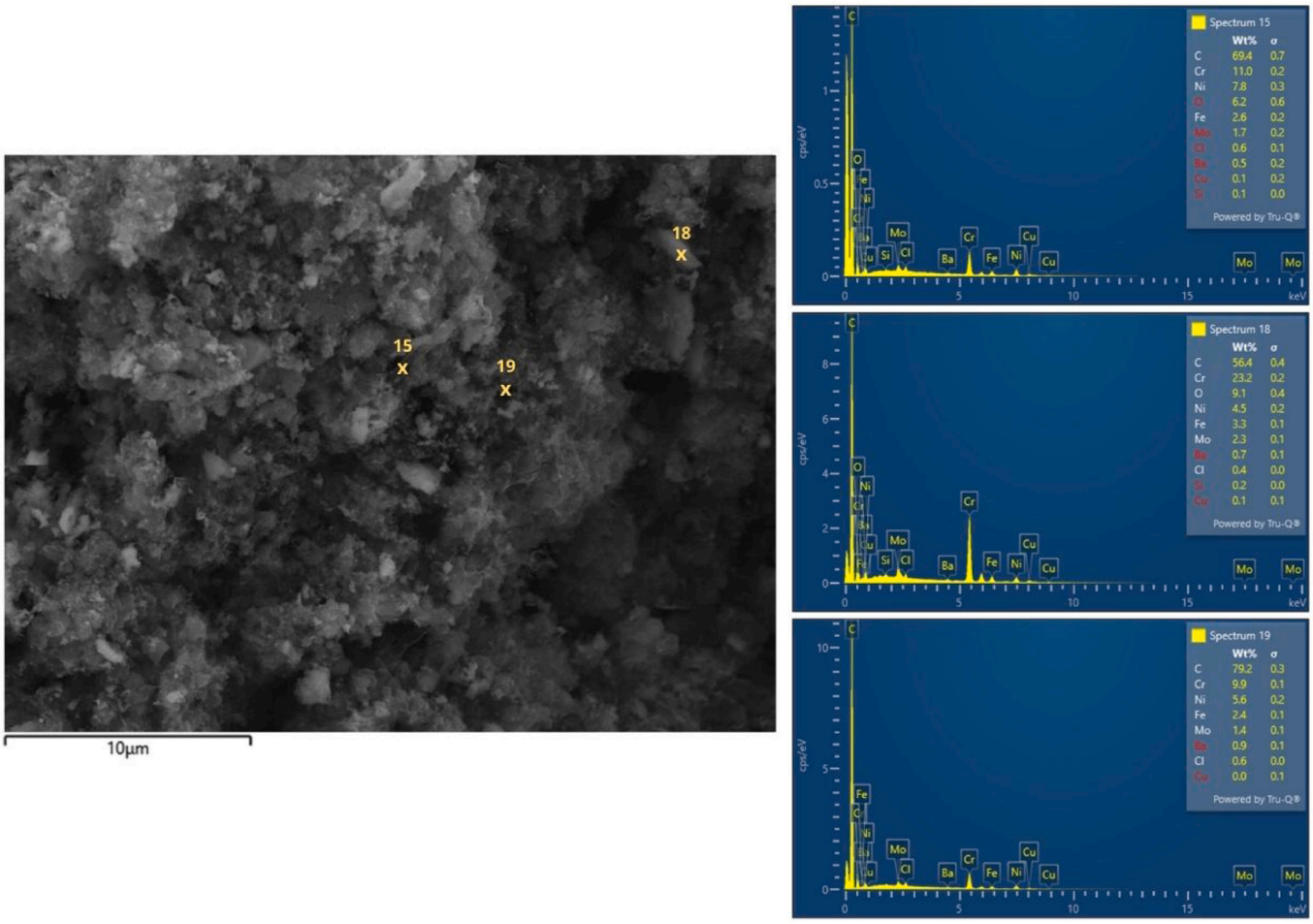

Fig. 7. EDS spectra of carbon produced in Li_2CO_3-$BaCO_3$ at 775 °C temperature.

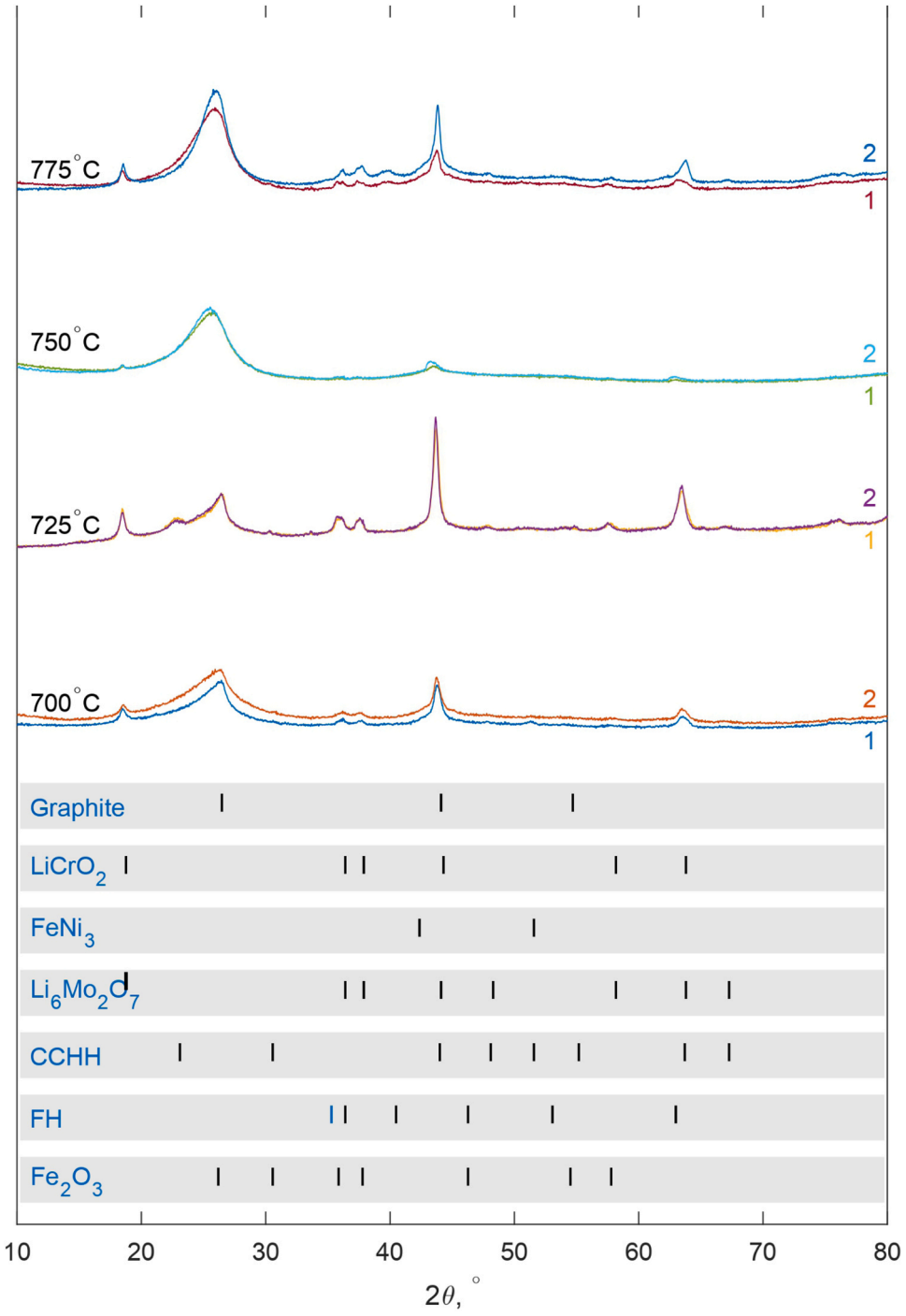

Fig. 8. XRD diffraction patterns of carbon samples produced at different temperatures in Li_2CO_3-$CaCO_3$ electrolyte. Number on the right side of the figure is equal to the number of the repetition. CCHH = Chromium chloride hexahydrate, FH = Ferrihydrite.

Table 4
Phase composition analysis (w%) of the samples from Li_2CO_3-$CaCO_3$ electrolyte based on reference intensity ratio (RIR) analysis.

Sample	Graphitic C	$LiCrO_2$	$FeNi_3$	$Li_6Mo_2O_7$	Fe_2O_3	CCHH	FH	Unidentified component
Li_2CO_3-$CaCO_3$ 700, rep1	76.5	12.2	1.6	9.7		–	–	1.7
Li_2CO_3-$CaCO_3$ 700, rep2	83.8	5.7	0.8	9.7		–	–	1.4
Li_2CO_3-$CaCO_3$ 725, rep1	56.1	14.7	0.3	18.7		10.1	–	0.5
Li_2CO_3-$CaCO_3$ 725, rep2	59.7	14.2	0.5	19.1		6.5	–	1.0
Li_2CO_3-$CaCO_3$ 750, rep1	95.9	0.7	–	3.3		–	–	2.0
Li_2CO_3-$CaCO_3$ 750, rep2	94.9	0.2	–	4.9		–	–	2.4
Li_2CO_3-$CaCO_3$ 775, rep1	87.9	4.1	–	5.2	0.7	–	2.1	1.4
Li_2CO_3-$CaCO_3$ 775, rep2	81.5	10.0	–	6.3	0.1	–	2.2	1.4

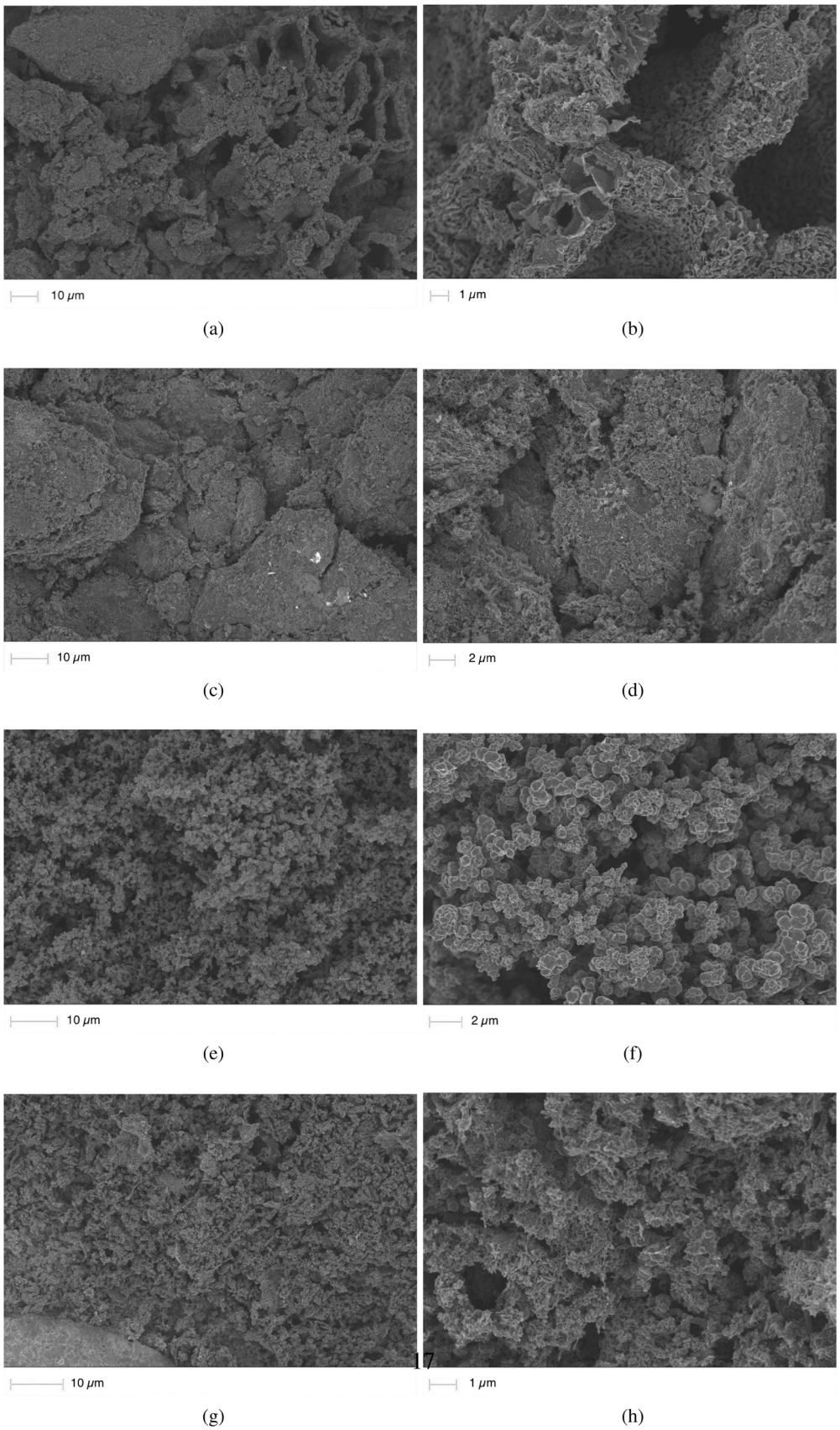

Fig. 9. Carbon produced at a)-b) 700 °C c)-d) 725 °C e)-f) 750 °C g)-h) 775 °C temperature in Li_2CO_3-$CaCO_3$ electrolyte. Electrolysis time in all the experiments was 90 min, and current density 0.2 A cm^{-2}.

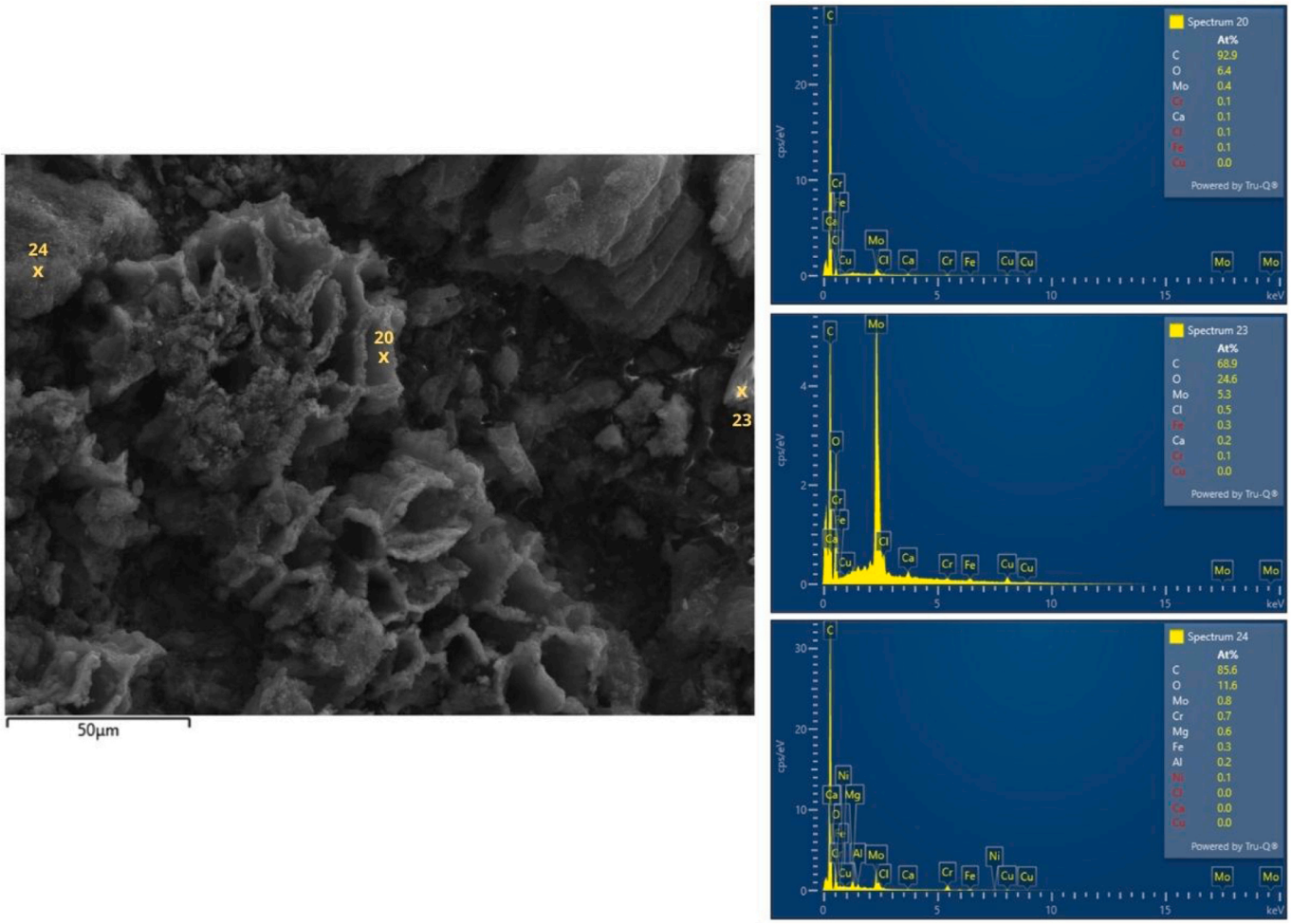

Fig. 10. EDS spectra of carbon produced in Li_2CO_3-$CaCO_3$ at 700 °C temperature.

3.2. *Electrolysis energy consumption, losses, and voltage efficiency*

Average cell voltages during the 90 min 10 A constant current electrolysis at in are shown in Fig. 14. The average cell voltage at 750 °C in pure lithium carbonate, here 1.92 V, is used as a reference case, as pure Li_2CO_3 is the most commonly utilized electrolyte in this type electrochemical splitting of CO_2. While temperature is increased the cell voltage decreased as expected. In the case of Li_2CO_3-$CaCO_3$ the effect of temperature to cell voltage was more significant compared to Li_2CO_3-$BaCO_3$. At 750 °C and 775 °C the average cell voltages were close to each other in all the experiments. Higher cell voltages result in elevated overpotential losses and lower voltage efficiency, which, in terms of energy consumption, are unfavorable. These losses contribute to an increase in the electrolysis power and subsequently energy consumption. Evaluating electrolysis power and energy consumption, the electrolysis is crucial for the possible consideration of an industrial scale system.

Electrolysis power and heat generation are shown in Fig. 15. Electrolysis power is higher at lower temperatures, and in Li_2CO_3-$CaCO_3$ electrolyte the effect of temperature to electrolysis power is greater. Observed overpotential losses manifest as heat production. Previously heat generation and overpotential loss during this type of molten salt electrolysis has been discussed in [2]. Heat generation is evident across all electrolytes at all studied temperatures. In industrial processes, heat generation plays a crucial role, affecting the overall system temperature. The results of this paper have shown that the electrolysis temperature has a significant effect on the product morphology, and thus maintaining electrolysis temperature constant is crucial in order to obtain good control over the product. To prevent undesired temperature change due to heat production temperature must be measured during the electrolysis, and subsequently heating power of the oven must be controlled.

4. Conclusions

The effect of electrolyte selection and electrolysis temperature to produced carbon morphology and electrolysis energy consumption and voltage efficiency were studied. Li_2CO_3-$BaCO_3$ 80:20 mol% and Li_2CO_3-$CaCO_3$ 80:20 mol% electrolytes were utilized at 700 °C, 725 °C, 750 °C, and 775 °C temperature in 10 A (0.2 A cm^{-2}) constant current electrolysis.

Based on the comprehensive analysis of the produced carbon, it is evident that both electrolyte composition and electrolysis temperature affect the carbon morphology. At 700 °C and 725 °C the product morphology differed significantly between the electrolytes, while at 750 °C and 775 °C structural similarities were found between samples produced with different electrolytes. Based on XRD diffraction patterns, it can be concluded that not only the morphology of the carbon changes, but also the type and amount of the metallic impurities change. The amount and number of different impurity components were significantly higher in the samples produced in Li_2CO_3-$BaCO_3$ compared to samples from Li_2CO_3-$CaCO_3$.

It can be concluded that the combination of Li_2CO_3-$BaCO_3$ electrolyte with Alloy X electrodes is unfavorable for this electrochemical process, particularly with regard to product purity. If future investigations would focus on Li_2CO_3-$BaCO_3$ electrolyte, alternative electrode materials such as titanium or platinum may yield superior outcomes by reducing the quantity and number of different impurities.

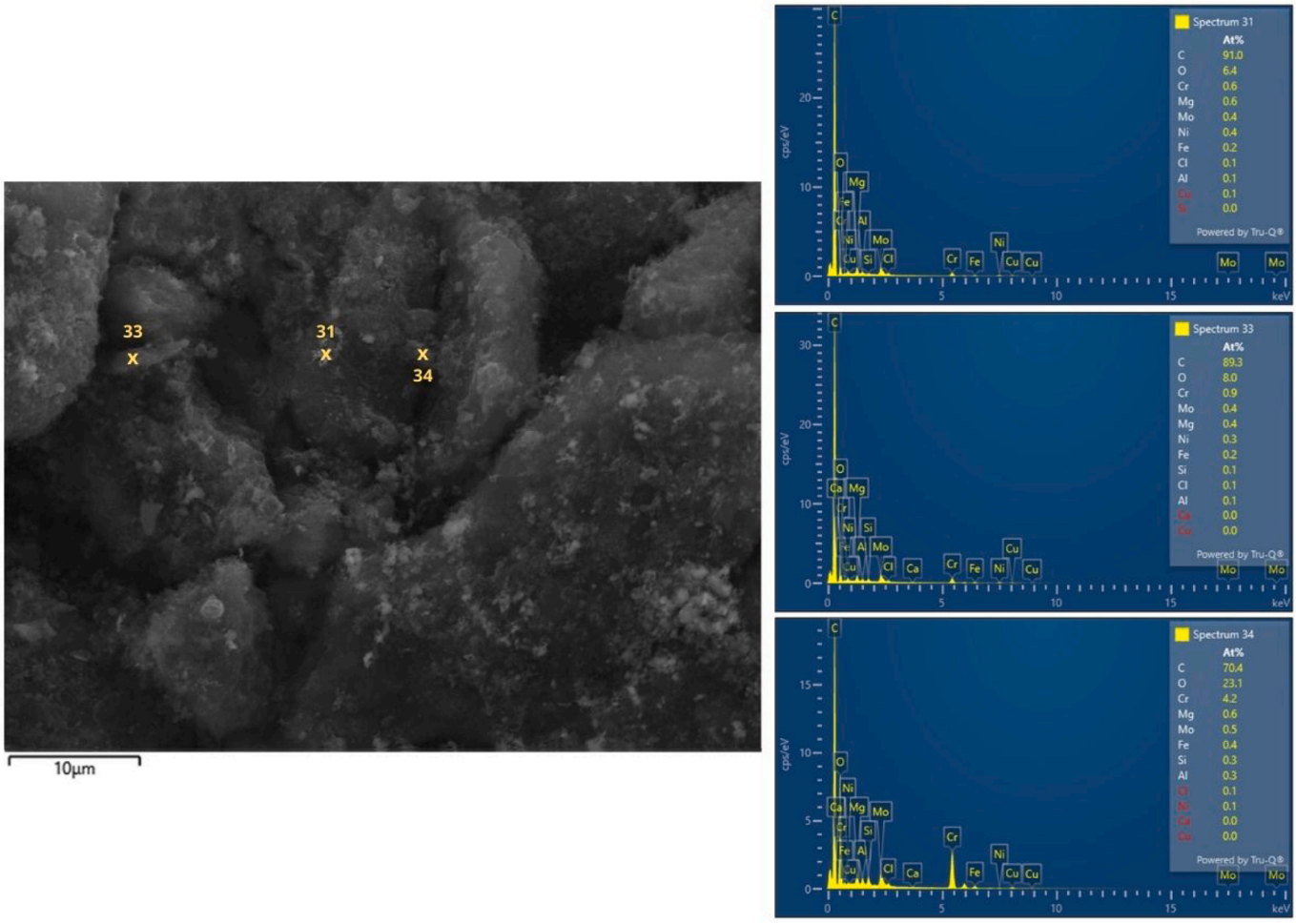

Fig. 11. EDS spectra of carbon produced in Li_2CO_3-$CaCO_3$ at 725 °C temperature.

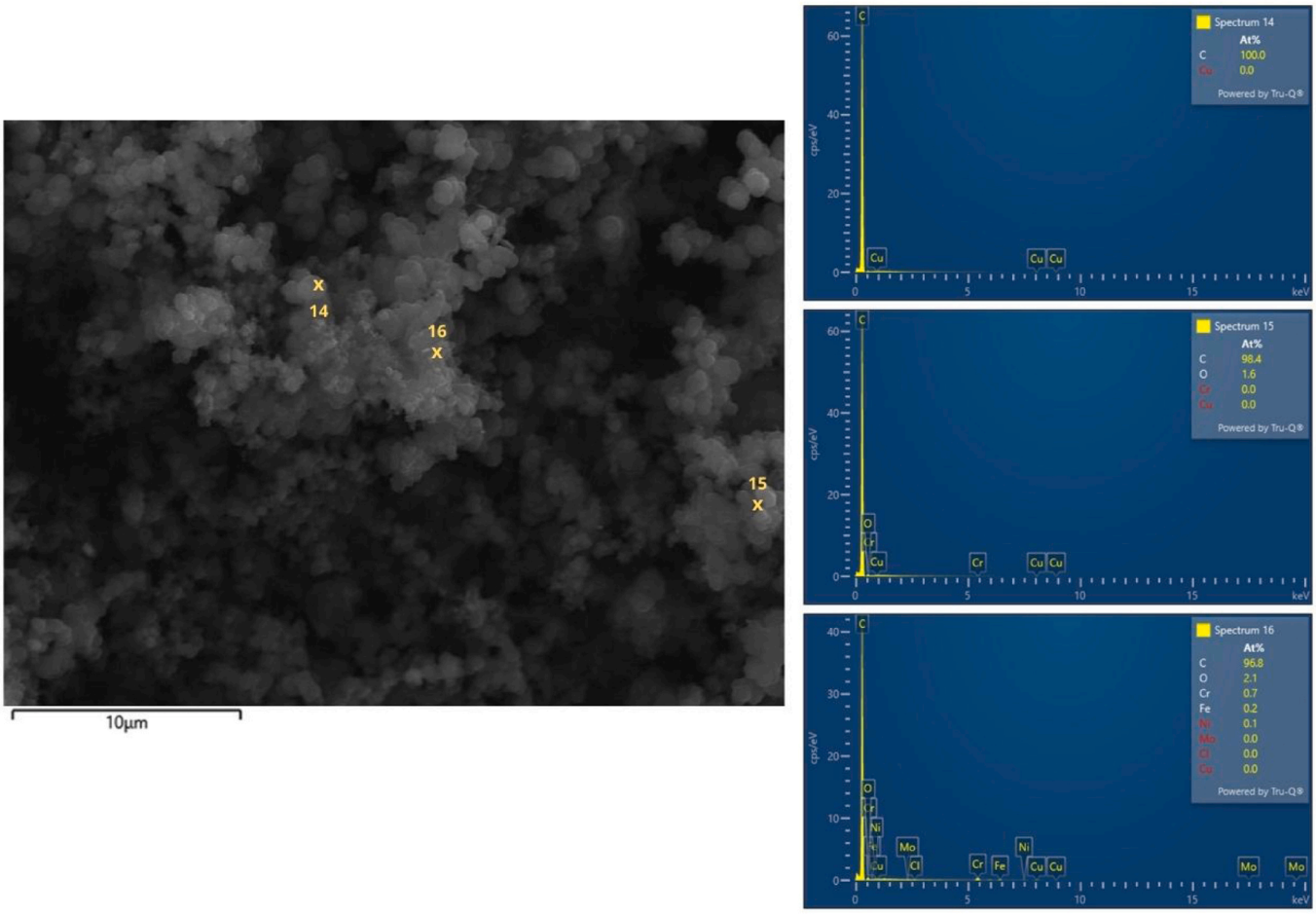

Fig. 12. EDS spectra of carbon produced in Li_2CO_3-$CaCO_3$ at 750 °C temperature.

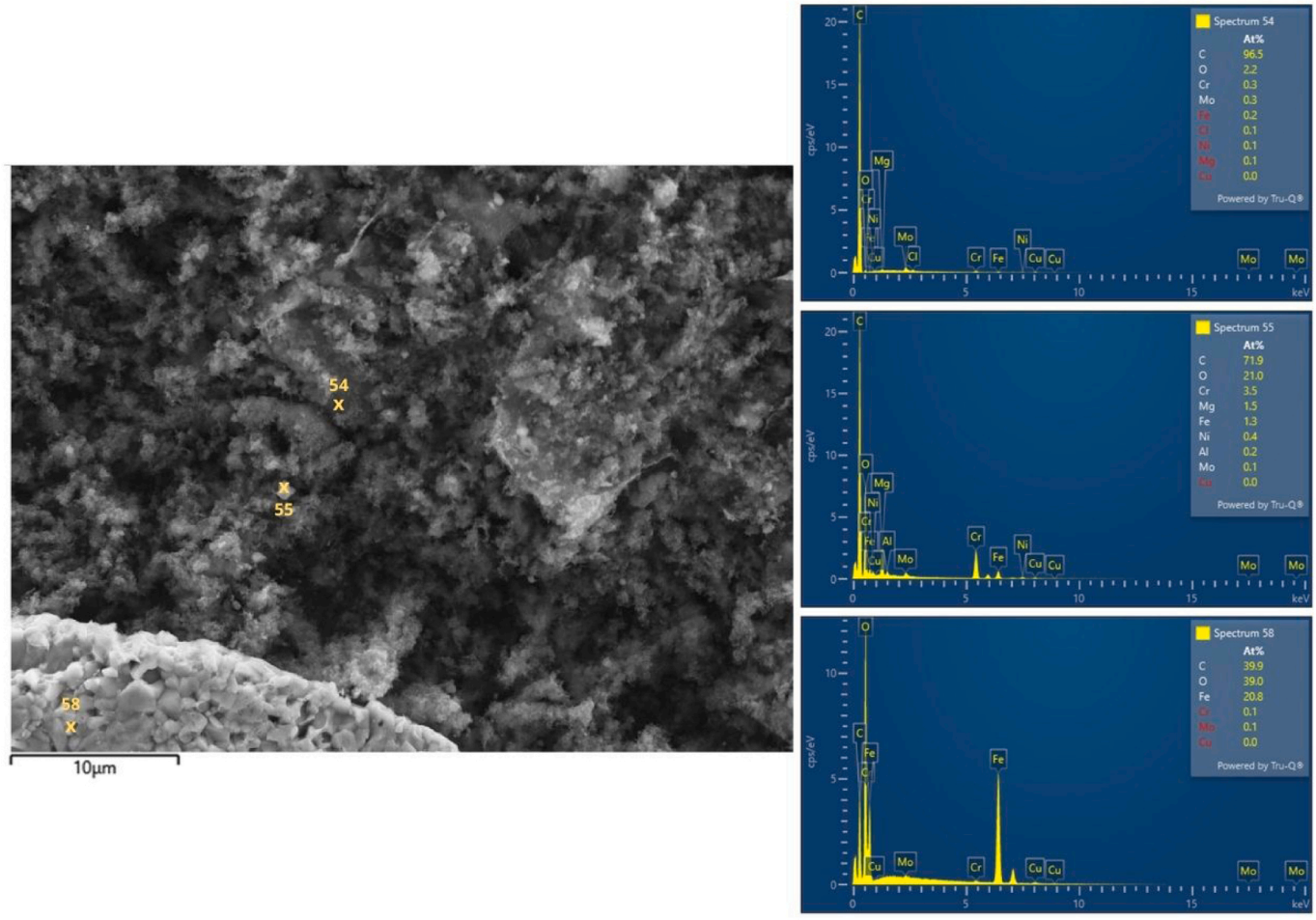

Fig. 13. EDS spectra of carbon produced in Li_2CO_3-$CaCO_3$ at 775 °C temperature.

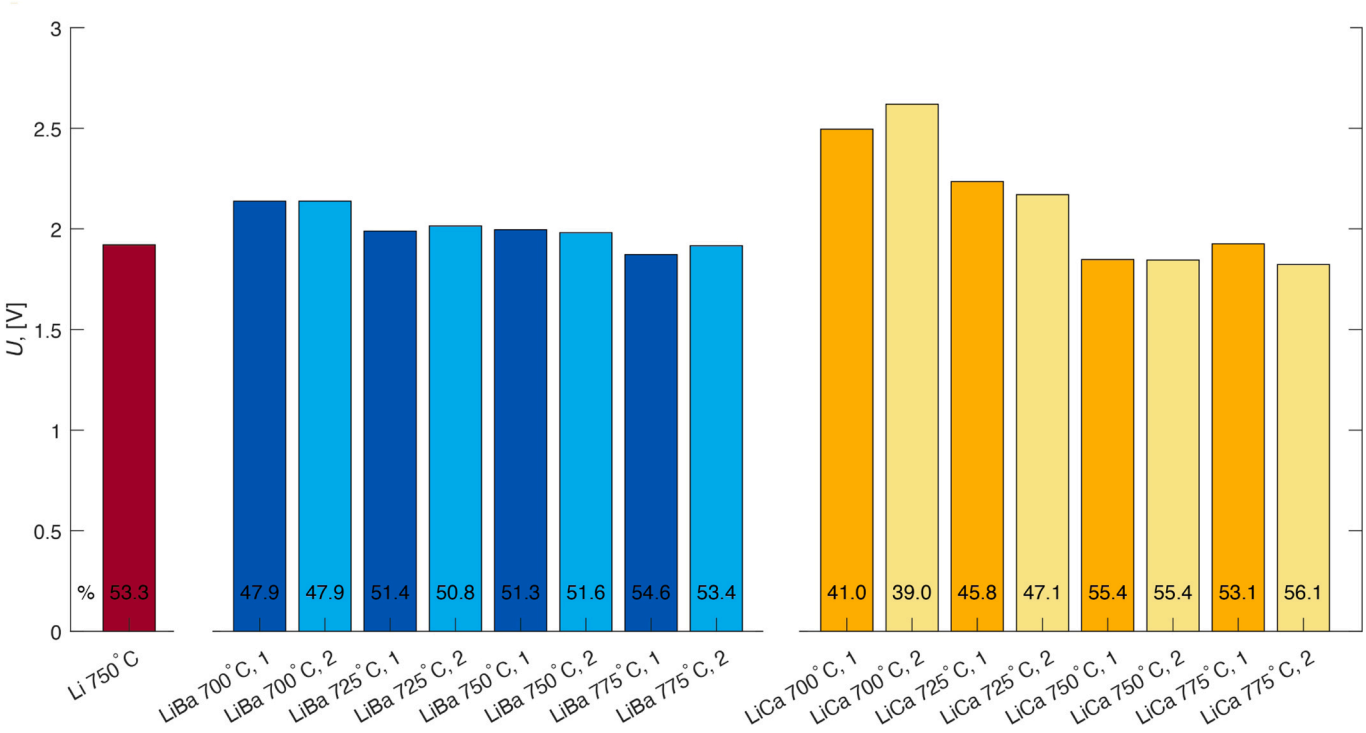

Fig. 14. Average cell voltages measured during the 90 min 10 A constant current electrolysis. Electrolysis voltage efficiency is shown as a number in the bars.

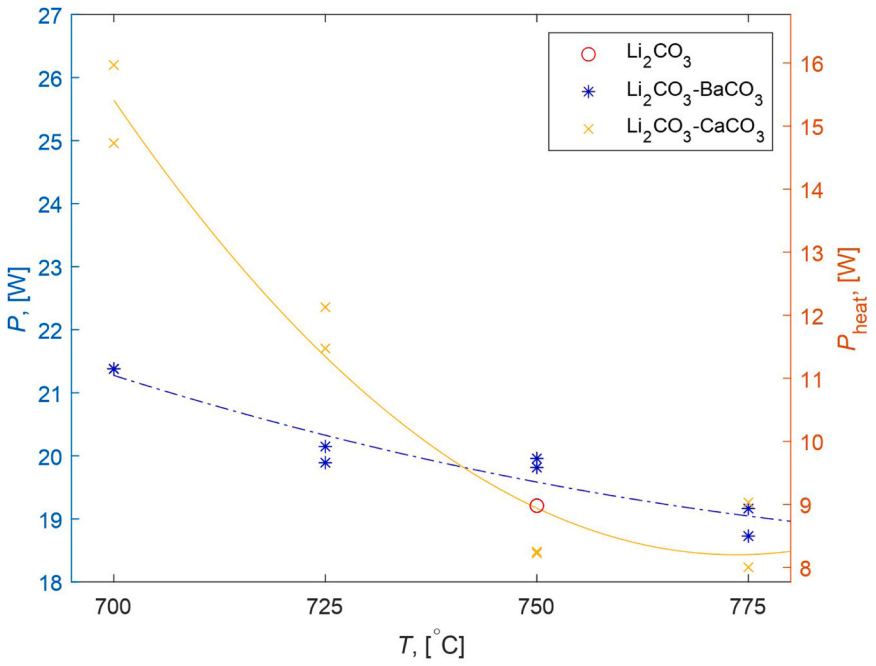

Fig. 15. Electrolysis power (left axis) and heat generation (right axis).

The results obtained with Li_2CO_3-$CaCO_3$ electrolyte are more promising. It could be advantageous in subsequent studies to explore different electrode materials and electrolysis temperatures within this specific electrolyte, or adjust the proportions of electrolyte components to further enhance the purity and quality of the resulting carbon.

In terms of energy consumption and voltage efficiency, Li_2CO_3-$CaCO_3$ is equal or slightly superior at temperatures 750 °C and beyond, compared to pure Li_2CO_3 and Li_2CO_3-$BaCO_3$. In terms of heat generation during the electrolysis, neither of the electrolyte options presented are optimal, as heat generation is observed in all the cases. In industrial processes, heat generation plays a crucial role as it can affect the overall system temperature. The results shown here emphasize the importance of maintaining a constant electrolysis temperature. To prevent unwanted temperature fluctuations caused by heat production, controlling the heating power of the oven is crucial in ensuring stable temperature during the electrolysis process.

Declaration of Competing Interest

The authors declare that they have no known competing financial interests or personal relationships that could have appeared to influence the work reported in this paper.

Acknowledgments

Jane and Aatos Erkko Foundation and the Technology Industries of Finland Centennial Foundation are acknowledged for financial support of the Neo-Carbon Materials project and Business Finland is acknowledged for financial support of the HYGCEL Hydrogen and Carbon Value Chains in Green Electrification project. The SEM imaging was performed at Tampere Microscopy Center facilities at Tampere University.

The author's would like to thank the staff of LUT Voima for their input on the experimental setup design and construction.

References

[1] X. Liu, J. Ren, G. Licht, X. Wang, S. Licht, Carbon nano-onions made directly from CO_2 by molten electrolysis for greenhouse gas mitigation, Adv. Sustain. Syst. 3 (10) (2019) 1900056, https://doi.org/10.1002/adsu.201900056.

[2] E. Laasonen, V. Ruuskanen, M. Niemelä, T. Koiranen, J. Ahola, Insights into carbon production by CO_2 reduction in molten salt electrolysis in coaxial-type reactor, J. Environ. Chem. Eng. 10 (1) (2022) 106933, https://doi.org/10.1016/j.jece.2021.106933.

[3] M. Johnson, J. Ren, M. Lefler, G. Licht, J. Vicini, X. Liu, S. Licht, Carbon nanotube wools made directly from CO_2 by molten electrolysis: value driven pathways to carbon dioxide greenhouse gas mitigation, Mater. Today Energy 5 (2017) 230–236, https://doi.org/10.1016/j.mtener.2017.07.003.

[4] J. Ren, F.-F. Li, J. Lau, L. González-Urbina, S. Licht, One-pot synthesis of carbon nanofibers from CO_2, Nano Lett. 15 (9) (2015) 6142–6148, https://doi.org/10.1021/acs.nanolett.5b02427.

[5] E. Laasonen, M. Sorvali, V. Ruuskanen, M. Niemelä, T. Koiranen, J. Ahola, J. M. Mäkelä, T. Joronen, The effect of metal dissolution on carbon production by high-temperature molten salt electrolysis, J. CO_2 Util. 69 (2023) 102390, https://doi.org/10.1016/j.jcou.2023.102390.

[6] S. Licht, A. Douglas, J. Ren, R. Carter, M. Lefler, C.L. Pint, Carbon nanotubes produced from ambient carbon dioxide for environmentally sustainable lithium-ion and sodium-ion battery anodes, ACS Cent. Sci. (2016) 162–168, https://doi.org/10.1021/acscentsci.5b00400.

[7] X. Liu, X. Wang, G. Licht, S. Licht, Transformation of the greenhouse gas carbon dioxide to graphene, J. CO_2 Util. 36 (2020) 288–294, https://doi.org/10.1016/j.jcou.2019.11.019.

[8] H. Wu, Z. Li, D. Ji, Y. Liu, L. Li, D. Yuan, Z. Zhang, J. Ren, M. Lefler, B. Wang, S. Licht, One-pot synthesis of nanostructured carbon materials from carbon dioxide via electrolysis in molten carbonate salts, Carbon 106 (2016) 208–217, https://doi.org/10.1016/j.carbon.2016.05.031.

[9] K. Le Van, H. Groult, F. Lantelme, M. Dubois, D. Avignant, A. Tressaud, S. Komaba, N. Kumagai, S. Sigrist, Electrochemical formation of carbon nano-powders with various porosities in molten alkali carbonates, Electrochim. Acta 54 (19) (2009) 4566–4573, https://doi.org/10.1016/j.electacta.2009.03.049.

[10] D. Tang, H. Yin, X. Mao, W. Xiao, D.H. Wang, Effects of applied voltage and temperature on the electrochemical production of carbon powders from CO_2 in molten salt with an inert anode, Electrochim. Acta 114 (2013) 567–573, https://doi.org/10.1016/j.electacta.2013.10.109.

[11] H.V. Ijije, C. Sun, G.Z. Chen, Indirect electrochemical reduction of carbon dioxide to carbon nanopowders in molten alkali carbonates: Process variables and product properties, Carbon 73 (2014), https://doi.org/10.1016/j.carbon.2014.02.052.

[12] X. Wang, G. Licht, X. Liu, S. Licht, One pot facile transformation of CO_2 to an unusual 3-D nano-scaffold morphology of carbon, Sci. Rep. 10 (1) (2020) 21518, https://doi.org/10.1038/s41598-020-78258-6.

[13] Z. Li, G. Wang, W. Zhang, Z. Qiao, H. Wu, Carbon nanotubes synthesis from CO_2 based on the molten salts electrochemistry: effect of alkaline earth carbonate additives on the diameter of the carbon nanotubes, J. Electrochem. Soc. 166 (10) (2019) D415, https://doi.org/10.1149/2.0861910jes.

[14] J. Ren, M. Johnson, R. Singhal, S. Licht, Transformation of the greenhouse gas CO_2 by molten electrolysis into a wide controlled selection of carbon nanotubes, J. CO_2 Util. 18 (2017) 335–344, https://doi.org/10.1016/j.jcou.2017.02.005.

[15] L. Li, W. Wong-Ng, K. Huang, L.P. Cook, L.P. Cook, Materials and Processes for CO_2 Capture, Conversion, and Sequestration (Incorporated, Newark, UNITED STATES), John Wiley & Sons, 2018.

[16] Z. Li, D. Yuan, H. Wu, W. Li, D. Gu, A novel route to synthesize carbon spheres and carbon nanotubes from carbon dioxide in a molten carbonate electrolyzer, Inorg. Chem. Front 5 (1) (2018) 208–216, https://doi.org/10.1039/C7QI00479F.
[17] M.A. Hughes, J.A. Allen, S.W. Donne, The properties of carbons derived through the electrolytic reduction of molten carbonates under varied conditions: Part I. A study based on step potential electrochemical spectroscopy, J. Electrochem. Soc. 165 (11) (2018) A2608, https://doi.org/10.1149/2.0351811jes.
[18] P. Wang, M. Wang, J. Lu, Electrochemical conversion of CO_2 into value-added carbon with desirable structures via molten carbonates electrolysis, RSC Adv. 11 (46) (2021) 28535–28541, https://doi.org/10.1039/D1RA03890G.
[19] Y. Yu, Z. Li, W. Zhang, W. Li, D. Ji, Y. Liu, Z. He, H. Wu, Effect of $BaCO_3$ addition on the CO_2 -derived carbon deposition in molten carbonates electrolyzer, N. J. Chem. 42 (2) (2018) 1208–1215, https://doi.org/10.1039/C7NJ03546B.
[20] P. Peng, A. Yu, J. Ren, F. Li, Electrolytic carbons from CO_2 and their applications, ESEE 2018 (2018) 9–20, https://doi.org/10.30919/esee8c205.
[21] P.K. Lorenz, G.J. Janz, Electrolysis of molten carbonates: anodic and cathodic gas-evolving reactions, Electrochim. Acta 15 (6) (1970) 1025–1035, https://doi.org/10.1016/0013-4686(70)80042-1.
[22] H.E. Bartlett, K.E. Johnson, Electrolytic reduction and ellingham diagrams for oxy-anion systems, Can. J. Chem. 44 (18) (1966) 2119–2129, https://doi.org/10.1139/v66-321.
[23] M.D. Ingram, B. Baron, G.J. Janz, The electrolytic deposition of carbon from fused carbonates, Electrochim. Acta 11 (11) (1966) 1629–1639, https://doi.org/10.1016/0013-4686(66)80076-2.
[24] A. Douglas, R. Carter, N. Muralidharan, L. Oakes, C. Pint, Iron catalyzed growth of crystalline multi-walled carbon nanotubes from ambient carbon dioxide mediated by molten carbonates, Carbon 116 (2017) 572–578, https://doi.org/10.1016/j.carbon.2017.02.032.
[25] S. Arcaro, F.A. Berutti, A.K. Alves, C.P. Bergmann, MWCNTs produced by electrolysis of molten carbonate: characteristics of the cathodic products grown on galvanized steel and nickel chrome electrodes, Appl. Surf. Sci. 466 (2019) 367–374, https://doi.org/10.1016/j.apsusc.2018.10.055.
[26] H. Ijije, G. Chen, Electrochemical manufacturing of nanocarbons from carbon dioxide in molten alkali metal carbonate salts: roles of alkali metal cations, Adv. Manuf. 4 (2016), https://doi.org/10.1007/s40436-015-0125-2.
[27] X. Liu, G. Licht, X. Wang, S. Licht, Controlled transition metal nucleated growth of carbon nanotubes by molten electrolysis of CO2, Catal. 12 (2) (2022) 137, https://doi.org/10.3390/catal12020137.
[28] Z. Li, Y. Yu, W. Li, G. Wang, L. Peng, J. Li, D. Gu, D. Yuan, H. Wu, Carbon dioxide electrolysis and carbon deposition in alkaline-earth-carbonate-included molten salts electrolyzer, N. J. Chem. 42 (19) (2018) 15663–15670, https://doi.org/10.1039/C8NJ02965B.
[29] K. Moyer, M. Zohair, J. Eaves-Rathert, A. Douglas, C.L. Pint, Oxygen evolution activity limits the nucleation and catalytic growth of carbon nanotubes from carbon dioxide electrolysis via molten carbonates, Carbon 165 (2020) 90–99, https://doi.org/10.1016/j.carbon.2020.04.037.
[30] J.E. House. Inorganic Chemistry, 2nd Edition, Academic Press, 2012.